A doubly distorted-wave method for atomic ionization by ultrashort laser pulses

M S Gravielle[1], D G Arbó[1], J E Miraglia[1] and M F Ciappina[2]

[1] Instituto de Astronomía y Física del Espacio (CONICET-UBA), Casilla de correo 67, Sucursal 28, 1428 Buenos Aires, Argentina
[2] ICFO—Institut de Ciènces Fotòniques, 08860 Castelldefels (Barcelona), Spain

E-mail: msilvia@iafe.uba.ar

Abstract
We study a time-dependent distorted-wave formulation of atomic ionization by short laser pulses named the double-distorted Coulomb–Volkov (DDCV) approximation. The method takes into account the distortions introduced by the laser field in the initial and final channels, both by means of the Volkov phase. The DDCV model is applied to evaluate electron emission distributions for hydrogen atoms ionized by multi-cycle laser pulses. Results are compared with the predictions of an *exact* treatment based on the numerical solution of the time-dependent Schrödinger equation (TDSE) and with values derived from the standard Coulomb–Volkov (CV) approach, considering different intensities and frequencies of the laser field. Good agreement with the TDSE solution has been obtained for laser frequencies higher than 0.1 au, extending the range of applicability of the usual CV-type methods.

(Some figures in this article are in colour only in the electronic version)

1. Introduction

In the last decade, the fast development of laser technology has transformed the study of the interaction of coherent electromagnetic radiation with matter in an extraordinarily active field. In particular, for the case of atomic targets, an intense experimental and theoretical research involving laser pulses in the femto- (or even atto-) second time domain has been developed [1–3]. Among the theoretical methods introduced to describe the electronic transitions produced by ultrashort laser pulses we can mention the Coulomb–Volkov (CV) approximation which has become a useful tool to investigate the physics behind photoinduced ionization processes. It has been used to study different aspects of the photoelectron emission, like the role played by the residual target potential [4], photon effects in the tunnel regime [5], the interference effects originated by different release times of the emitted electron [6] and near threshold ionization structures in H_2^+ molecules [7].

The CV approximation is a time-dependent distorted-wave theory that makes use of the well-known CV wavefunction [8–12] to describe the action of the laser electric field on the active electron in the exit channel. In this way, the CV approach can be considered as a single-distorted method because it includes the distortion of the laser pulse only in the final state, while the initial channel is represented by the unperturbed atomic wavefunction in the absence of the external field. It has been shown that the CV approximation can provide accurate electron energy distributions for a large variety of laser pulses, ranging from non-oscillating to multi-cycle fields [13–15]. It represents a reliable alternative approach to the numerical solution of the time-dependent Schrödinger equation (TDSE) and other semiclassical models [16, 17], with the advantage that it can be easily extended for multi-electronic targets. Nevertheless, it fails when the perturbative conditions are not fulfilled (i.e. for intense laser fields for which the ionization is produced in an effective time much shorter than the pulse duration) or when the ionization requires multi-photon transitions through intermediate excited states, as it happens for photon energies smaller than the atomic ionization potential. Lately, an improvement on the standard CV approach was developed by Smirnova *et al* [18], which

is based on the use of the Coulomb–Eikonal–Volkov state to take into account both the depletion and the Stark shift of the ground state. Other modifications of the CV theory were introduced in [19–21] by expanding the initial state on a basis set of unperturbed atomic wavefunctions and then solving the close-coupling equations for their populations.

Alternatively, for the purpose of improving the description of the initial channel given by the CV approach, in a previous work [14] we introduced the double-distorted Coulomb–Volkov (DDCV) approximation, which includes the effect of the laser field on the initial and final states on an equal footing. The incorporation of the distortion produced by the laser in the initial channel accounts for dynamic Stark effects (energy and wavefunction time-dependent modifications), which are expected to play an important role for high values of the quiver amplitude of the laser electric field [14]. The DDCV method has been successfully employed to study the ionization of atomic hydrogen by half-cycle laser pulses, displaying an improvement on the CV approach for high momentum transfers, especially in the region of low electron energies where the CV theory breaks down [22].

In this paper, we extend the application of the DDCV model to laser pulses involving several oscillations of the electric field inside the envelope. In order to test the performance of the DDCV approach for multi-cycle pulses we evaluate photoelectron emission spectra for hydrogen atoms, comparing them with *exact* calculations obtained from the numerical solution of the TDSE in three spatial dimensions [23]. Our aim is to derive a simple and realistic method that allows us to extract information about the different ionization mechanisms and can be straightforwardly extended to more complex systems [24–28], for which the applicability of the TDSE becomes computationally prohibitive.

The paper is organized as follows. In section 2, we derive the DDCV approximation from the time-dependent distorted wave formalism. Electron energy and momentum distributions for hydrogen ionization are presented in section 3, considering different field strengths and frequencies of the laser pulse. Finally, in section 4 we discuss our main conclusions. Atomic units are used throughout unless otherwise stated.

2. Theory

Let us consider a target atom T interacting with a time-dependent electric field $\mathbf{F}(t)$, which characterizes the laser pulse in the dipole approximation. As a consequence of this interaction, one electron e of the target, initially bound to the atomic nucleus in the state ϕ_i, is emitted in a continuum state ϕ_f with momentum $\mathbf{k}_f$. In the presence of the external electric field, the temporal evolution of the electronic state $\Psi(\mathbf{r}, t)$ is governed by the Schrödinger equation

$$i\frac{\partial \Psi(\mathbf{r}, t)}{\partial t} = [H_0 + V_L(\mathbf{r}, t)]\Psi(\mathbf{r}, t), \qquad (1)$$

where $H_0 = -\nabla_{\mathbf{r}}^2/2 + V_T(\mathbf{r})$ is the unperturbed atomic Hamiltonian, with $\mathbf{r}$ the position vector of the active electron e and V_T the electron-target potential, and the term $V_L(\mathbf{r}, t) = \mathbf{r} \cdot \mathbf{F}(t)$ represents the interaction potential with the laser field

expressed in the length gauge. For hydrogenic targets, like the ones considered here, $V_T(\mathbf{r}) = -Z/r$, Z being the nuclear charge ($Z = 1$ for hydrogen).

To describe the electron emission process we make use of the distorted-wave formulation [29, 30], which is based on the idea of taking account of a substantial part of the interaction potential by means of approximate wavefunctions. Within the framework of the time-dependent distorted-wave formalism [31], it is possible to derive a double-distorted theory by considering distorted wavefunctions χ_i and χ_f to represent the initial and final channels, respectively. The *post*(+) and *prior*(−) forms of the double-distorted T-matrix element read [14]

$$T_{if}^{\pm} = a_{if}^{\mp} - i \int_{-\infty}^{+\infty} dt \langle \chi_f(t) | \mathcal{W}^{\pm} | \chi_i(t) \rangle, \qquad (2)$$

where $\mathcal{W}^+ = W_f^{\dagger}(t)$ and $\mathcal{W}^- = W_i(t)$ are the final and initial distortion potentials, respectively, defined by $W_j(t) |\chi_j(t)\rangle = (H_0 + V_L(\mathbf{r}, t) - i\partial/\partial t)|\chi_j(t)\rangle$, with $j = i, f$. The first term of equation (2) corresponds to the transition amplitude in the *sudden* limit, which is expressed as

$$a_{if}^+ = \lim_{t \to +\infty} \langle \phi_f(t) | \chi_i(t) \rangle, \qquad post \text{ form}, \qquad (3)$$

$$a_{if}^- = \lim_{t \to -\infty} \langle \chi_f(t) | \phi_i(t) \rangle, \qquad prior \text{ form}. \qquad (4)$$

These sudden amplitudes provide the main contribution to the ionization probability when the duration of the pulse is much shorter than the orbital period of the electron in the initial state and consequently, the field becomes a sudden momentum transfer [10].

In this work, we use CV-type wavefunctions as initial and final distorted states. For the initial channel we propose the impulse Coulomb–Volkov (ICV) wavefunction [14], which is based on the impulsive hypothesis [30, 32] that states that the main effect of V_T is to determine the initial electron momentum distribution. This hypothesis is particularly valid for ultrashort laser pulses when the pulse duration is shorter than the characteristic time of the electron motion. Then, the ICV wavefunction is derived from the momentum distribution of the initial state ϕ_i by including the action of the laser field through the phase of the Volkov function [33]. The Volkov wavefunction represents the exact quantum state for a free electron moving in a time-dependent electric field and its phase has been extensively employed to study different radiation-matter problems [34–38]. The initial ICV wavefunction reads [14]

$$\chi_i \equiv \chi_i^{\text{ICV}+}(\mathbf{r}, t) = \frac{1}{(2\pi)^{3/2}} \int d\mathbf{k} \exp(-i\varepsilon_i t)\widetilde{\varphi}_i(\mathbf{k})$$
$$\times \exp[i\mathbf{k} \cdot \mathbf{r} + iD_L^+(\mathbf{k}, \mathbf{r}, t)]$$
$$= \phi_i[\mathbf{r} - \boldsymbol{\alpha}^+(t)] \exp[iD_L^+(\mathbf{0}, \mathbf{r}, t)], \qquad (5)$$

where $\phi_i(\mathbf{r}, t) = \exp(-i\varepsilon_i t)\varphi_i(\mathbf{r})$ is the initial bound state with energy ε_i and the tilde denotes the Fourier transformation in the momentum space. The Volkov phase is expressed as

$$D_L^{\pm}(\mathbf{k}, \mathbf{r}, t) = \mathbf{A}^{\pm}(t) \cdot \mathbf{r} - \beta^{\pm}(t) - \mathbf{k} \cdot \boldsymbol{\alpha}^{\pm}(t), \qquad (6)$$

where

$$\mathbf{A}^{\pm}(t) = -\int_{\mp\infty}^{t} dt' \mathbf{F}(t'),$$

$$\beta^{\pm}(t) = 2^{-1} \int_{\mp\infty}^{t} dt' [\mathbf{A}^{\pm}(t')]^2, \qquad (7)$$

$$\boldsymbol{\alpha}^{\pm}(t) = \int_{\mp\infty}^{t} dt' \mathbf{A}^{\pm}(t')$$

are associated with the vector potential, the ponderomotive energy and the quiver amplitude, respectively.

In a similar way, in the final channel we employ the usual CV state [8]

$$\chi_f \equiv \chi_f^{\mathrm{CV}-}(\mathbf{r}, t) = \phi_f(\mathbf{r}, t) \exp[i D_L^-(\mathbf{k}_f, \mathbf{r}, t)], \qquad (8)$$

where $\phi_f(\mathbf{r}, t) = \varphi_f^-(\mathbf{r}) \exp(-i\varepsilon_f t)$ is the final Coulomb wavefunction with momentum $\mathbf{k}_f$ and energy $\varepsilon_f = k_f^2/2$, with

$$\varphi_f^-(\mathbf{r}) = (2\pi)^{-3/2} \exp(i\mathbf{k}_f \cdot \mathbf{r}) \mathcal{D}^-(Z, \mathbf{k}_f, \mathbf{r}), \qquad (9)$$

$$\mathcal{D}^-(Z, \mathbf{k}_f, \mathbf{r}) = \exp(\pi\nu_f/2)\Gamma(1 + i\nu_f)$$
$$\times \, _1F_1\left(-i\nu_f, 1, -ik_f \, r - i\mathbf{k}_f \cdot \mathbf{r}\right), \qquad (10)$$

$\nu_f = Z/k_f$, $_1F_1$ the confluent hypergeometric function and $k_f = |\mathbf{k}_f|$. The proposed initial and final distorted wavefunctions (equations (5) and (8)) satisfy the proper asymptotic conditions, i.e. $\chi_i^{\mathrm{ICV}+}(t) \to \phi_i(t)$ for $t \to -\infty$ and $\chi_f^{\mathrm{CV}-}(t) \to \phi_f(t)$ for $t \to +\infty$, regarded $A^{\pm}(t) \to 0$ as $t \to \mp\infty$, respectively.

For hydrogenic targets, for which ϕ_i and ϕ_f are exact eigenfunctions of the atomic Hamiltonian H_0, both forms of the transition matrix are equivalent, i.e. $T_{if}^- = T_{if}^+$. But for multi-electronic atoms, a *post–prior* discrepancy arises when a Hartree–Fock wavefunction is considered to represent the initial bound state while the final one is described using an effective Coulombic charge. In such cases, the use of the *prior* expression should be more appropriate [39] because it includes the initial distortion potential W_i, which does not depend on the choice of the effective charge. Here, for the sake of simplicity we summarize only the expression of the *post* form, which was employed in the calculations of this paper. Replacing $\chi_i^{\mathrm{ICV}+}$ and $\chi_f^{\mathrm{CV}-}$ in equation (2), the *post* DDCV transition amplitude reads

$$T_{if}^{(\mathrm{DDCV})+} = e^{i\delta(t_0)} L_i[\mathbf{k}_f, \mathbf{p}(t_0), \mathbf{0}] + \int_{-\infty}^{+\infty} dt \, e^{i\delta(t)}$$
$$\times \, \mathbf{N}_i[\mathbf{k}_f, \mathbf{p}(t), \mathbf{d}(t)] \cdot \mathbf{A}^-(t), \qquad (11)$$

where t_0 denotes the time when the pulse is turned on, $\mathbf{p}(t) = \mathbf{k}_f + \Delta\mathbf{A}(t)$, $\mathbf{d}(t) = \boldsymbol{\alpha}^+(t)$ and

$$\delta(t) = \Delta\epsilon \, t + \Delta\beta(t) + \mathbf{k}_f \cdot \boldsymbol{\alpha}^-(t), \qquad (12)$$

with $\Delta\epsilon = \varepsilon_f - \varepsilon_i$, $\Delta\beta(t) = \beta^-(t) - \beta^+(t)$ and $\Delta\mathbf{A}(t) = \mathbf{A}^-(t) - \mathbf{A}^+(t)$. The functions $L_i[\mathbf{k}, \mathbf{q}, \mathbf{d}]$ and $\mathbf{N}_i[\mathbf{k}, \mathbf{q}, \mathbf{d}]$ are Nordsieck integrals [30], being defined as

$$\begin{Bmatrix} L_i[\mathbf{k}, \mathbf{q}, \mathbf{d}] \\ \mathbf{N}_i[\mathbf{k}, \mathbf{q}, \mathbf{d}] \end{Bmatrix} = \int d\mathbf{r} \frac{\exp(-i\mathbf{q} \cdot \mathbf{r})}{(2\pi)^{3/2}} \varphi_i(\mathbf{r} - \mathbf{d})$$
$$\times \begin{Bmatrix} 1 \\ \nabla_{\mathbf{r}} \end{Bmatrix} \mathcal{D}^{-*}(Z, \mathbf{k}, \mathbf{r}). \qquad (13)$$

For $\mathbf{d} = \mathbf{0}$, these functions reduce to one-centre integrals, presenting closed analytical forms [40]. But when the displacement $\mathbf{d}$ is not null, as it happens in the second term of equation (11), they involve two-centre integrals which must be numerically evaluated. Note that the CV transition matrix [13, 14] can be obtained from equation (11) by neglecting the Volkov phase in the initial channel; that is, by fixing $\mathbf{A}^+(t) = \boldsymbol{\alpha}^+(t) = 0$ and $\beta^+(t) = 0$.

3. Results

The DDCV approximation is applied to study electron emission from H(1s) produced by the incidence of a linearly polarized laser pulse. As hydrogen is the simplest atomic target, with only one bound electron, this system will be considered as a benchmark for the theory. The temporal profile of the laser electric field $\mathbf{F}(t)$ is chosen as

$$F(t) = F_0 \sin(\omega t + \varphi) \sin^2(\pi t/\tau) \qquad (14)$$

for $0 < t < \tau$ and 0 elsewhere, where F_0 is the maximum field strength, ω is the carrier frequency, τ determines the pulse duration and the carrier envelope phase is defined as $\varphi = -\omega\tau/2 + \pi/2$ to obtain a symmetric pulse, i.e.
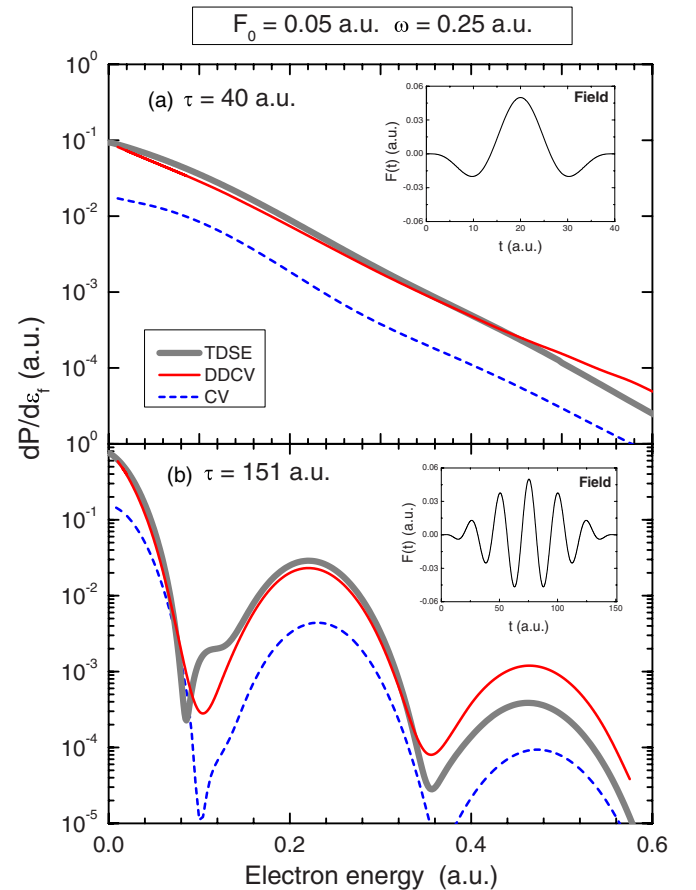

Figure 1. Electron energy spectra for hydrogen ionization obtained from TDSE (grey thick line), DDCV (red solid line), and CV (blue dashed line) calculations. The laser parameters are $F_0 = 0.05$ au and $\omega = 0.25$ au. The duration of the pulse is (a) $\tau = 40$ au and (b) $\tau = 151$ au. Insets: corresponding laser electric fields, as a function of the time.
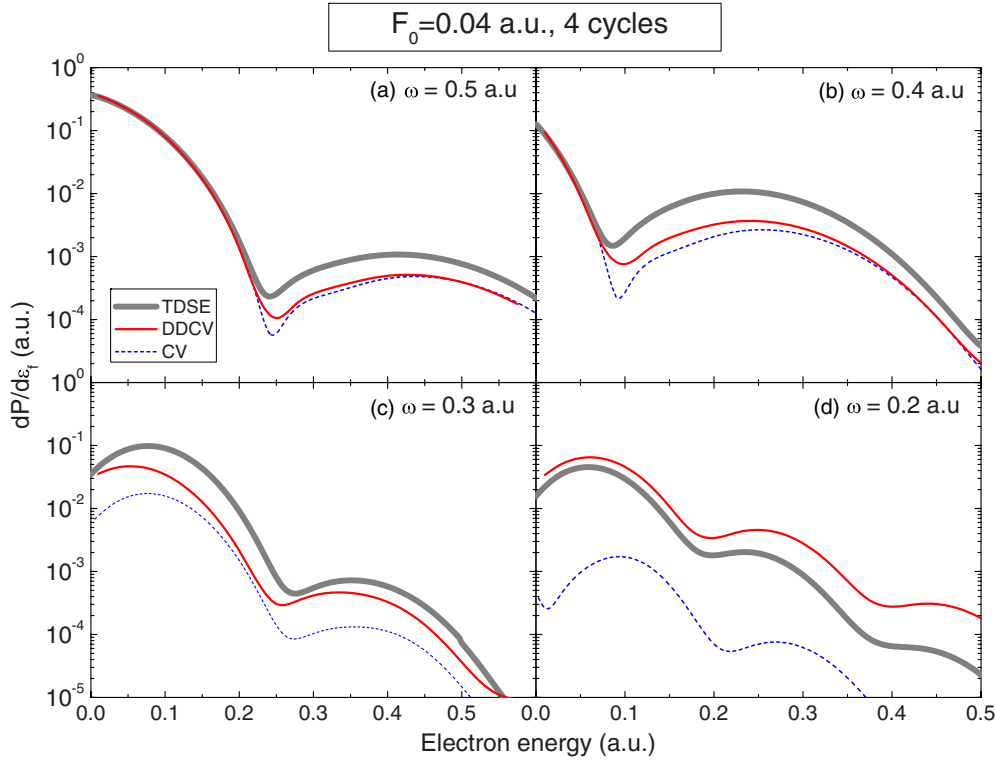
Figure 2. Same as figure 1 for a four-cycle laser pulse with $F_0 = 0.04$ au. The laser frequency of the pulse is (a) $\omega = 0.5$ au, (b) $\omega = 0.4$ au, (c) $\omega = 0.3$ au and (d) $\omega = 0.2$ au.

$F(t) = F(\tau - t)$. For pulses containing an integer number of cycles inside the envelope, the duration of the pulse is $\tau = n\, 2\pi/\omega$, with n the number of cycles.

Within the DDCV approach the energy distribution of the emitted electrons can be derived from $T_{if}^{(DDCV)+}$ by integrating over the direction of the ejected electron

$$\frac{\mathrm{d}P_{if}^{(DDCV)}}{\mathrm{d}\varepsilon_f} = k_f \int \mathrm{d}\Omega_f \left| T_{if}^{(DDCV)+} \right|^2, \qquad (15)$$

where Ω_f is the solid angle determined by the final electron momentum $\mathbf{k}_f$. To calculate $T_{if}^{(DDCV)+}$ the three-dimensional integral involved in the definition of $\mathbf{N}_i[\mathbf{k}, \mathbf{q}, \mathbf{d}]$ (equation (13)) was numerically solved in the momentum space with a relative error lower than 1%, while the further integration on time was calculated with a relative error lower than 0.1%, after appropriately checking the numerical convergence. In addition, from equation (12) it should be noted that the DDCV T-matrix element includes the ponderomotive energy shift in the initial and final channels both in an equivalent way, leading to a total energy shift $\Delta\beta(t)$ that is constant in the case of oscillating pulses that fulfil the condition of travelling waves, i.e. $\mathbf{A}^+(\tau) = 0$. Therefore, in order to take into account that the electron is less sensitive to the energy shift produced by external field in the initial bound state than in the nearly free final continue state, in the evaluation of equation (11) we have introduced an additional approximation by dropping the term $\beta^+(t)$ in the time-dependent phase $\delta(t)$.[3]

---

[3] For travelling waves the inclusion of $\beta^+(t)$ in $\Delta\beta(t)$, as given by equation (12), introduces a unrealistic energy shift of multi-photon maxima.

Electron energy distributions obtained from equation (15) are compared with those derived from the single-distorted CV approach and with the numerical solution of the TDSE. The TDSE was solved by means of the generalized pseudo-spectral method [23] that combines a discretization of the radial coordinate optimized for the Coulomb singularity with quadrature methods to achieve stable long-time evolution using a split-operator technique. The method allows for an accurate description of both the unbound and the bound parts of the total wavefunction $\Psi(\mathbf{r}, t)$. Details of the calculations can be found in [23].

We start studying the ionization from the ground state of H originated by an electromagnetic field with $F_0 = 0.05$ au and $\omega = 0.25$ au (that corresponds to a laser intensity $I = 8.78 \times 10^{13}\ \mathrm{W\,cm^{-2}}$ and a wavelength $\lambda = 182.2$ nm, respectively). In figure 1, two different regimes (pulse durations) are considered: (a) the collisional regime ($\tau = 40$ au), for which the laser field does not oscillate and resembles a classical field produced by the impact of a charged projectile, and (b) the multi-cycle regime ($\tau = 151$ au), for which the laser field performs several oscillations inside the envelope ($n = 6$ cycles). In both situations—collisional and multi-cycle—the DDCV approximation is in good accord with TDSE calculations, correcting the large underestimation displayed by the CV approach. However, in spite of the overall good agreement, DDCV results run slightly over the TDSE curve for high electron velocities in the multi-cycle regime (figure 1(b)), in the energy region where the ionization probability has decreased several orders of magnitude. This discrepancy might be related to the fact that at high electron

J. Phys. B: At. Mol. Opt. Phys. **45** (2012) 015601

M S Gravielle *et al*

energies the effects of the residual target and laser potentials on the released electron are not equivalent; consequently, they should be described in a different way. Maxima of figure 1(b) correspond to above-threshold-ionization (ATI) peaks produced by the absorption of an integer number of photons from the initial ground state and their energy positions are well described by the DDCV approach. But in addition, the TDSE spectrum displays a small structure at $E \simeq 0.11$ au, which stems from one-photon ionization from the 2p state. Both CV and DDCV approaches are unable to tackle this effect.

In order to study the behaviour of the proposed DDCV approach within the multi-cycle regime, in figure 2 we consider photoemission spectra for four-cycle ($n = 4$) laser pulses with a fixed intensity of the field ($I = 5.62 \times 10^{13}$ W cm^{-2}, i.e. $F_0 = 0.04$ au), decreasing the frequency from $\omega = 0.5$ au ($\lambda = 91.1$ nm) to $\omega = 0.2$ au ($\lambda = 227.8$ nm). Considering that the main difference between the DDCV and CV approaches lies on the inclusion of the quiver amplitude $\alpha^+(t)$ in the initial distorted state, we analyse the different cases in terms of the parameter $\alpha_0 = F_0/\omega^2$ which provides a measure of the maximum value of $|\alpha^+|$ for multi-cycle pulses. For $\omega = 0.5$ au both distorted-wave methods—DDCV and CV—provide a good description of the TDSE electron distribution, being very similar to each other. This is so because the parameter α_0 that characterizes the quiver amplitude ($\alpha_0 = 0.16$ au) is negligible with respect to the mean radius of the initial electronic distribution. The same behaviour is observed for $\omega > 0.5$ au: CV, DDCV and TDSE spectra become almost indistinguishable among them as the frequency increases. But when ω diminishes and consequently α_0 augments, the DDCV theory remains fairly close to the *exact* values derived from the TDSE method, departing from the CV curve that largely underestimates the electron emission probability for $\omega = 0.2$ au ($\alpha_0 = 1$ au). As mentioned in section 1, the standard CV approximation fails to reproduce TDSE results for $\omega < |\varepsilon_i|$, which for hydrogen targets is $|\varepsilon_i| = 0.5$ au, as a consequence of the absence of intermediate excited states, which contribute to the multi-photon absorption processes [15]. This deficiency of the CV theory is partially remedied in the DDCV approach by including the quiver amplitude in the initial channel. Since $\alpha^+(t)$ represents the classical displacement of the free electron from its centre of oscillation in a radiation field, its incorporation to the initial wavefunction ϕ_i as a displacement term allows the DDCV model to take into account, albeit partially, the Stark mixing of the initial state. However, for laser frequencies $\omega \leqslant 0.1$ au the DDCV approximation starts to fail, giving rise to unreliable electron emission spectra.

In figure 3, we consider hydrogen ionization by four-cycle ($n = 4$) laser pulses with a fixed value of $\alpha_0 = F_0/\omega^2 = 2$ au and different frequencies, varying accordingly the value of the peak laser electric field F_0. In all of the cases, even in those in which the perturbative conditions are not fulfilled (figures 3(a) and (b)), DDCV results are in fairly good agreement with the TDSE distributions and this agreement improves as the intensity of the field decreases. Note that the positions of the ATI maxima are well described by the DDCV
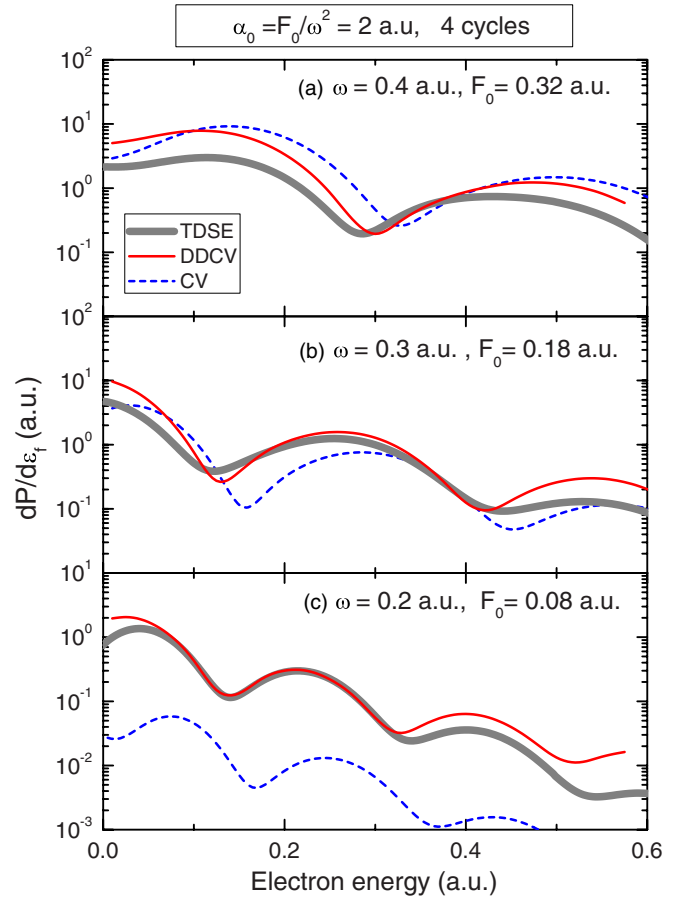

Figure 3. Same as figure 1 for a four-cycle laser pulse with $\alpha_0 = F_0/\omega^2 = 2$ au. The parameters of the laser field are (a) $\omega = 0.4$ au and $F_0 = 0.32$ au, (b) $\omega = 0.3$ au and $F_0 = 0.18$ au, and (c) $\omega = 0.2$ au and $F_0 = 0.08$ au.

curves, in contrast with the CV distributions which present peaks shifted with respect to the TDSE positions.

Finally, we analyse the electron momentum distributions corresponding to the electromagnetic fields of figures 3(a) and (c). In figure 4 two-dimensional spectra calculated within the CV and DDCV approximations, as a function of the components of the final electron momentum parallel ($k_\parallel$) and perpendicular ($k_\perp$) to the polarization direction of the external field, are compared with the ones derived from TDSE calculations. The three momentum distributions—TDSE, DDCV and CV—display similar features: radial lobes and annular structures at small and large $k_f = \sqrt{k_\parallel^2 + k_\perp^2}$ values, respectively. The ring-shaped patterns at larger k_f are related to the ATI peaks, while the lobular structures in the threshold region are just inside the first ATI ring, being focused by the Coulomb potential of the remaining target [4]. For $\omega = 0.4$ au, the CV and DDCV momentum distributions are similar to the one obtained from the TDSE solution. They present three lobes at low k_f and such lobes show a right–left asymmetry, the right lobe being bigger than the left one, something also observed in the TDSE calculations. However, strong differences between CV and DDCV double differential probabilities arise as the frequency decreases. For the lower frequency, $\omega = 0.2$ au, the DDCV approach gives a good
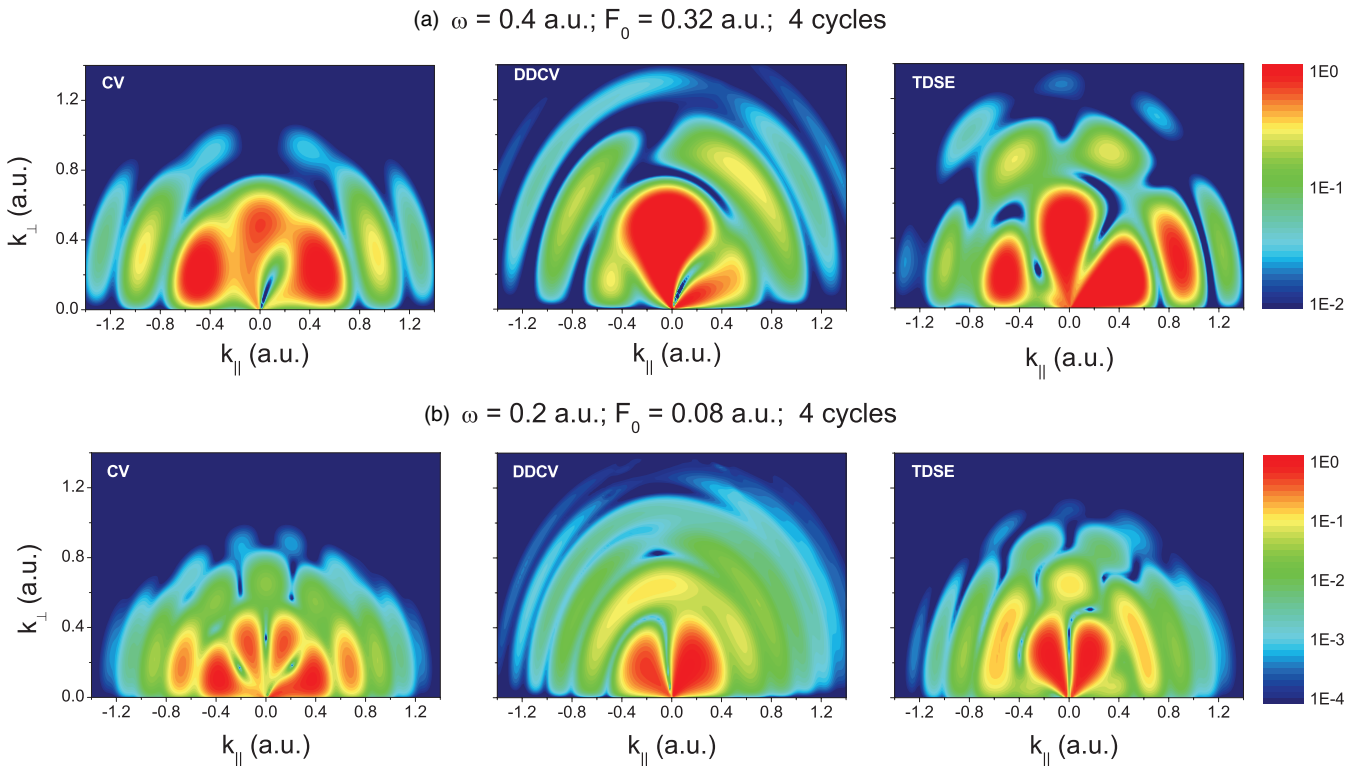
(a) ω = 0.4 a.u.; F$_0$ = 0.32 a.u.; 4 cycles

(b) ω = 0.2 a.u.; F$_0$ = 0.08 a.u.; 4 cycles

Figure 4. Double-differential electron momentum distributions (logarithmic scale) evaluated with the CV, DDCV and TDSE models, with respect to the final electron momenta parallel ($k_\parallel$) and perpendicular ($k_\perp$) to the laser field. The parameters of the four-cycle laser pulse are (a) $\omega = 0.4$ au and $F_0 = 0.32$ au, (b) $\omega = 0.2$ au and $F_0 = 0.08$ au. CV and DDCV distributions normalized to the total probability derived from TDSE calculations.

representation of the TDSE double differential distribution, both models displaying two lobes in the threshold region of the momentum spectrum. In contrast, the CV distribution presents four lobes at the threshold, in complete disagreement with the TDSE calculations.

4. Conclusions

We have investigated the DDCV approximation which includes the effect of the laser field in the initial and final channels. The DDCV model represents an improvement on the standard CV approach, converging towards the CV theory for small values of the quiver parameter α^+. In particular, we have found that for H (1s) ionization by multi-cycle laser pulses the DDCV approximation provides reliable predictions of the electron energy and momentum distributions in the range of laser frequencies 0.2 au $< \omega < 0.5$ au, where the CV approach is inadequate. When the frequency increases, becoming higher than the ionization energy $|\varepsilon_i| = 0.5$ au, both CV and DDCV results converge to the TDSE values. However, for $\omega \leqslant 0.1$ au the DDCV theory still fails to reproduce the electron spectra derived from TDSE calculations. This behaviour seems to be independent of the number of cycles inside the envelope of the laser field. We have not observed any considerable dependence of the level of agreement between DDCV and TDSE results on the total pulse duration, besides the inability of the former theory to track the depletion of the ground state.

References

[1] Milosevic D B, Paulus G G, Bauer D and Becker W 2006 *J. Phys. B: At. Mol. Opt. Phys.* **39** R203
[2] Scrinzi A, Yu Ivanov M, Kienberger R and Villeneuve D M 2006 *J. Phys. B: At. Mol. Opt. Phys.* **39** R1
[3] Krausz F and Ivanov M 2009 *Rev. Mod. Phys.* **81** 163
[4] Arbó D G, Miraglia J E, Gravielle M S, Schiessl K, Persson E and Burgdörfer J 2008 *Phys. Rev.* A **77** 013401
[5] Faisal F H M and Schlegel G 2005 *J. Phys. B: At. Mol. Opt. Phys.* **38** L223
[6] Arbó D G, Ishikawa K L, Schiessl K, Persson E and Burgdörfer J 2010 *Phys. Rev.* A **82** 043426
[7] Ciappina M F and Cravero W R 2009 *J. Mod. Opt.* **56** 11–56
   Ciappina M F and Cravero W R 2009 *J. Mod. Opt.* **82** 043426
[8] Jain M and Tzoar N 1978 *Phys. Rev.* A **18** 538
[9] Cavalieri P, Ferrante G and Leone C 1980 *J. Phys. B: At. Mol. Phys.* **13** 4495
[10] Duchateau G, Cormier E and Gayet R 2000 *Eur. Phys. J.* D **11** 191
   Duchateau G, Cormier E, Bachau H and Gayet R 2001 *Phys. Rev.* A **63** 053411
[11] Kornev A S and Zon B A 2002 *J. Phys. B: At. Mol. Opt. Phys.* **35** 2451

[12] Yudin G L, Patchkovskii S, Corkum P B and Bandrauk A D 2007 *J. Phys. B: At. Mol. Opt. Phys.* **40** F93

[13] Duchateau G, Cormier E and Gayet R 2002 *Phys. Rev.* A **66** 023412

[14] Macri P A, Miraglia J E and Gravielle M S 2003 *J. Opt. Soc. Am.* B **20** 1801

[15] Rodríguez V D, Cormier E and Gayet R 2004 *Phys. Rev. A* **69** 053402

[16] Lewenstein M, Balcou P, Yu Ivanov M, L'Huillier A and Corkum P B 1994 *Phys. Rev. A* **49** 2117

[17] Yan T-M, Popruzhenko S V, Vrakking M J J and Bauer D 2010 *Phys. Rev. Lett.* **105** 253002

[18] Smirnova O, Spanner M and Ivanov M 2006 *J. Phys. B: At. Mol. Opt. Phys.* **39** S307
Smirnova O, Spanner M and Ivanov M 2006 *J. Phys. B: At. Mol. Opt. Phys.* **39** S323

[19] Gayet R 2005 *J. Phys. B: At. Mol. Opt. Phys.* **38** 3905

[20] Gichard R and Gayet R 2006 *Phys. Rev.* A **74** 011402

[21] Rodríguez V D, Arbó D G and Macri P A 2011 *J. Phys. B: At. Mol. Opt. Phys.* **44** 125603

[22] Arbó D G, Gravielle M S, Dimitriou K I, Tőkési K, Borbély S and Miraglia J E 2010 *Eur. Phys. J.* D **59** 193

[23] Tong X-M and Chu S I 1997 *Chem. Phys.* **217** 119

[24] Baggesen J C and Madsen L B 2008 *Phys. Rev. A* **78** 032903

[25] Zhang C-H and Thumm U 2009 *Phys. Rev. Lett.* **102** 123601

[26] Zhang C-H and Thumm U 2009 *Phys. Rev.* A **80** 032902

[27] Faraggi M N, Aldazabal I, Gravielle M S, Arnau A and Silkin V M 2009 *J. Opt. Soc. Am.* B **26** 2331

[28] Acuña M A and Gravielle M S 2011 *Phys. Rev.* A **83** 032904

[29] Dodd L R and Greider K R 1966 *Phys. Rev.* **146** 675

[30] McDowell M R C and Coleman J P 1970 *Introduction to the Theory of Ion–Atom Collisions* (Amsterdam: North-Holland)

[31] Dewangan D P and Eichler J 1994 *Phys. Rep.* **247** 59

[32] Miraglia J E 1982 *J. Phys. B: At. Mol. Phys.* **15** 4205

[33] Volkov D M 1935 *Z. Phys.* **94** 250

[34] Reiss H R 1980 *Phys. Rev. A* **22** 1786

[35] Ivanov M, Corkum P B, Zuo T and Bandrauk A 1995 *Phys. Rev. Lett.* **74** 2933

[36] Jaron A, Kaminski J Z and Ehlotzky F 2000 *Phys. Rev.* A **61** 023404

[37] Becker A and Faisal F M 2005 *J. Phys. B: At. Mol. Opt. Phys.* **38** R1

[38] Milosevic D B, Paulus G G and Becker W 2003 *Opt. Express* **11** 1418

[39] Monti J M, Fojón O A, Hanssen J and Rivarola R D 2010 *J. Phys. B: At. Mol. Opt. Phys.* **43** 205203

[40] Gravielle M S and Miraglia J E 1992 *Comput. Phys. Commun.* **69** 53